

# Supporting Information for

## **Ion-Induced Nanopatterning of Bacterial Cellulose Hydrogels for Biosensing and Anti-Biofouling Interfaces**

Sandra L. Arias<sup>1†\*</sup>, Ming Kit Cheng<sup>2†</sup>, Ana Civantos<sup>2</sup>, Joshua Devorkin<sup>2</sup>, Camilo Jaramillo<sup>2</sup>,  
Jean Paul Allain<sup>1, 2 \*</sup>

<sup>1</sup>Department of Bioengineering, University of Illinois at Urbana-Champaign, IL 61801

<sup>2</sup>Department of Nuclear, Plasma and Radiological Engineering, University of Illinois at Urbana-Champaign, IL 61801

† Equal contributions

\*Correspondence to [slarias@cornell.edu](mailto:slarias@cornell.edu), [allain@psu.edu](mailto:allain@psu.edu)

### **This PDF file includes:**

Supplementary Text  
Figs. S1 to S5  
References (43-46)

## Supplementary text

### Raman spectroscopy confirmed the formation of graphite-like clusters in bacterial cellulose

The Raman spectrum indicated the typical bands for BC (**Fig. S5 A**). The bands in the region below 1500  $\text{cm}^{-1}$  are associated with the deformations of the internal coordinates of the anhydroglucopyranose residues, whereas those above 1500  $\text{cm}^{-1}$  are dominated by CH,  $\text{CH}_2$ , and OH stretching vibrations<sup>43,44</sup>. In the low frequency region for the pristine BC, the Raman pattern shows two intense bands at 576 and 1091  $\text{cm}^{-1}$ , and a medium-weak intensity band at 434  $\text{cm}^{-1}$ . All these bands exhibit a reduction in intensity with increasing argon dose. The band at 434  $\text{cm}^{-1}$  is associated with ring deformations of the glucopyranose skeletons and bending motions of glycosidic linkages (CCC, CCO). The band at 576  $\text{cm}^{-1}$  is also dominated by vibrational modes of the glucopyranose ring units (COC). Similarly, the band located at 1091  $\text{cm}^{-1}$  is characterized by vibrational modes involving CC and CO stretching motions, often coupled to glucopyranose ring breathing<sup>44</sup>. This indicates that bond breaking took place mainly at these locations in the hydrogel, which is probably responsible for the ring opening and chain-breaking phenomenon observed in the XPS spectra. In contrast, in the high frequency region above 1000  $\text{cm}^{-1}$ , a band center about 1570  $\text{cm}^{-1}$  emerged with increasing  $\text{Ar}^+$  dose, and which is absent in the pristine sample (**Fig. S5 B**). This band is associated with the G peak in amorphous carbons and suggests the presence of C sp<sup>2</sup> atoms in olefinic chains or conjugated carbon chains<sup>45,46</sup>. Another feature in amorphous carbons is the presence of a D band about 1350  $\text{cm}^{-1}$ , which is strictly linked to presence of six-fold aromatic rings<sup>46</sup>. In the region between 1270-1500  $\text{cm}^{-1}$ , native celluloses also exhibit several closely spaced, medium-intensity bands that correspond to internal coordinates of CCH, OCH, COH, and HCH bending motions<sup>43</sup>. The existence of these medium-intensity bands makes difficult the examination of the D-peak as a function of the fluence, and the determination of the overall intensity ratio of the D and G peak. However, the presence of the G and D peaks indicate the formation of carbon clusters in the hydrogel upon irradiation. As mentioned above, this carbon clustering could be contributing to the mechanism responsible for nanopattern formation, the increase in material stiffness, and the observed resilience of the nanostructures to capillary force. Finally, the high-intensity band at 2895  $\text{cm}^{-1}$  associated with stretching vibration of CH and  $\text{CH}_2$  bonds<sup>43</sup> (**Fig. S5**), decreased in intensity upon irradiation, suggesting that dehydrogenation may be linked to ion irradiation.

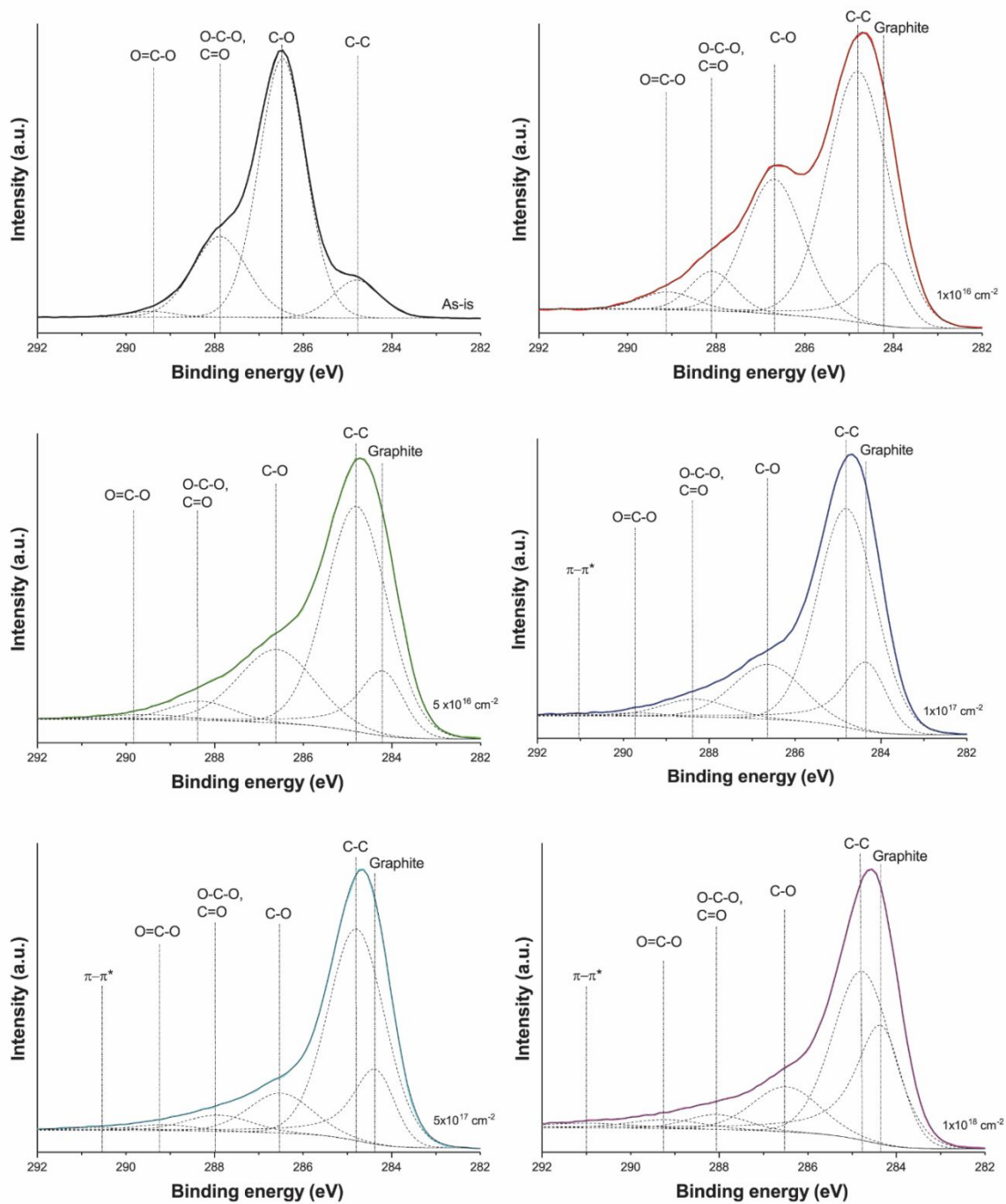


**Fig. S1.** Deconvolution of the C1s peak of pristine BC and argon-irradiated BC at increasing ion fluence

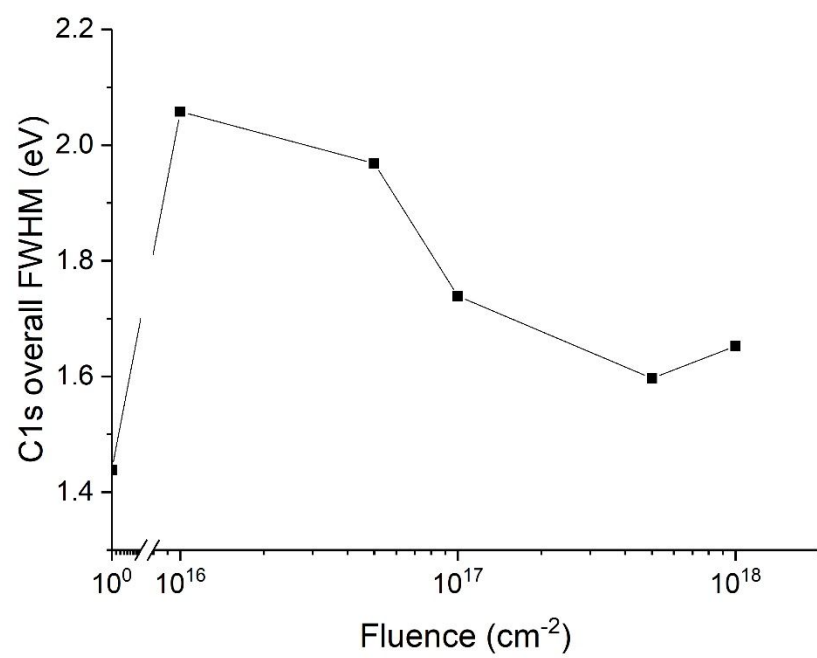


Fig. S2. FWHM of the C1s peak for BC as a function of the fluence

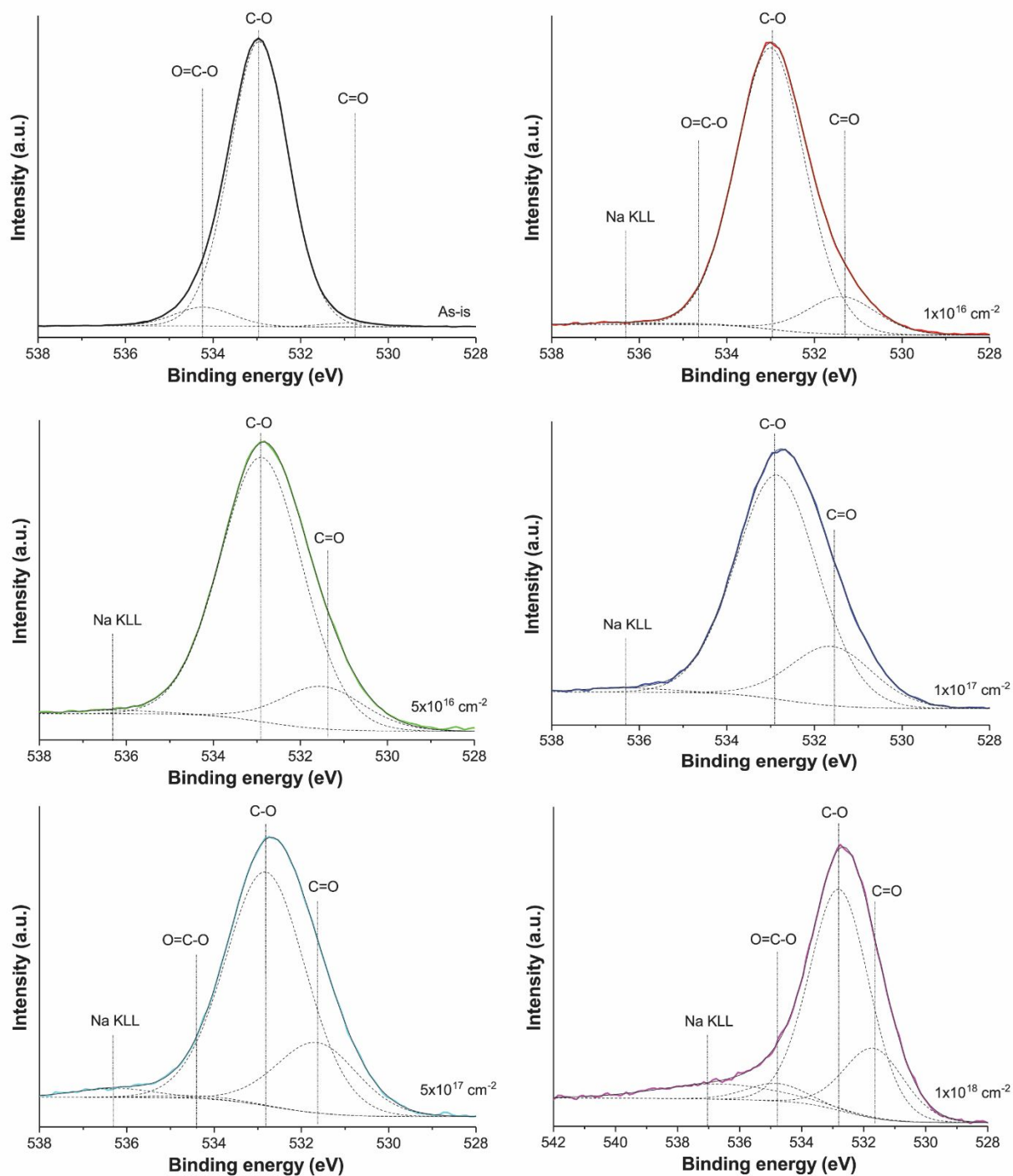
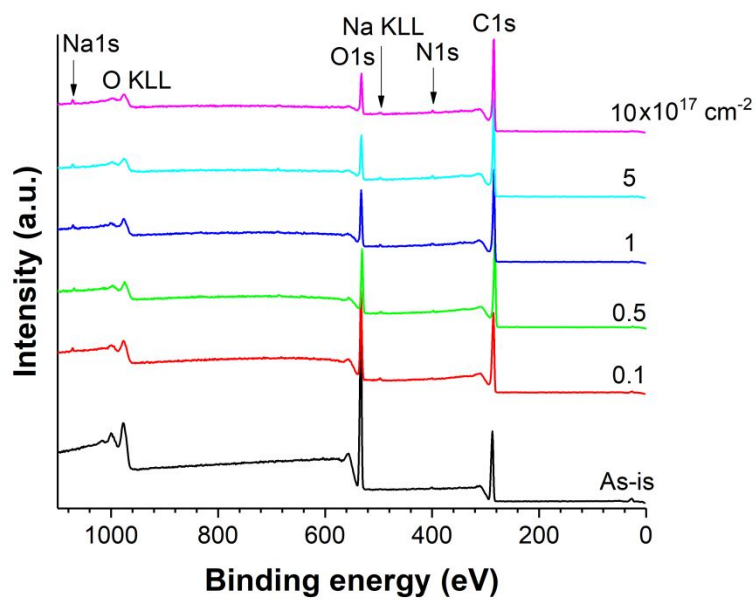
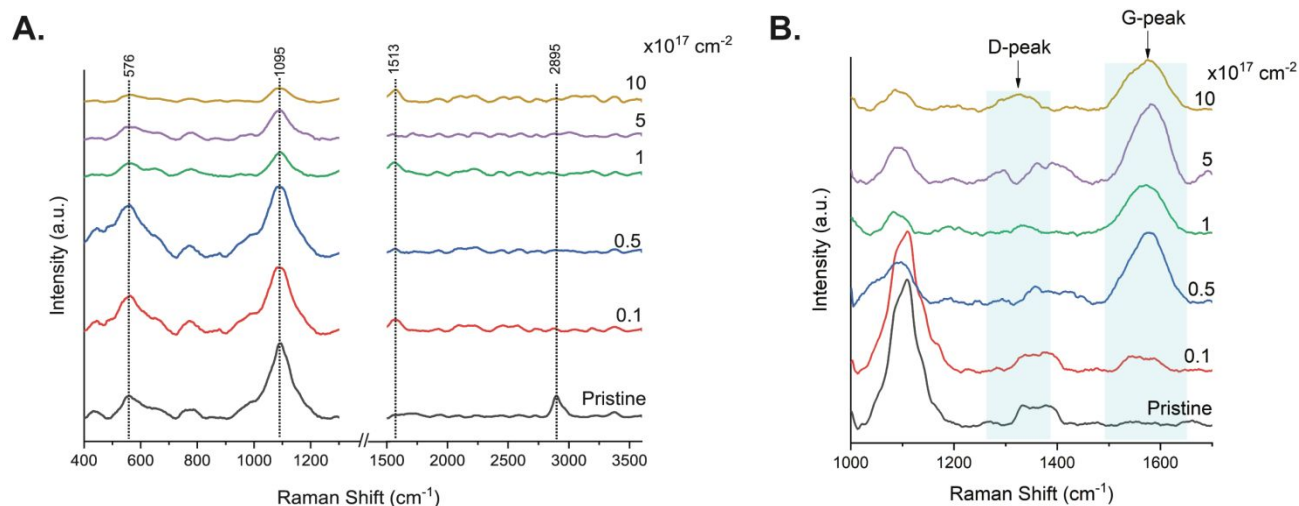


Fig. S3. Deconvolution of O1s peak of pristine BC and argon-irradiated BC at increasing ion fluences



**Fig. S4.** Wide spectrum of pristine and Ar-irradiated BC at increasing ion fluence, showing the slight presence of Na.



**Fig. S5.** Raman patterns confirm the presence of amorphous carbon in BC upon low-energy argon irradiation. Measured Raman spectra of pristine and argon-irradiated BC collected at an excitation wavelength of 532 nm. **(A)** In the low frequency region (400-1200  $\text{cm}^{-1}$ ), the spectrum shows a reduction in intensity for the most intense bands at 576, 1091  $\text{cm}^{-1}$ , and 434  $\text{cm}^{-1}$  in pristine BC with increasing ion dose. Those bands are associated with vibrational and breathing modes of the glucopyranose ring units. **(B)** Closer examination of the 100-1600  $\text{cm}^{-1}$  region shows the formation of graphite-like structures upon argon irradiation, which are associated with a G and D peak at about 1570  $\text{cm}^{-1}$  and 1350  $\text{cm}^{-1}$ , respectively.

## References

43. Willey, J. H.; Atalla, R. H., Band assignments in the Raman spectra of celluloses. *Carbohydr. Res.* **1987**, *160*, 113-129.
44. Schenzel, K.; Fischer, S. NIR FT Raman spectroscopy—a rapid analytical tool for detecting the transformation of cellulose polymorphs. *Cellulose* **2001**, *8*, 49-57.
45. Schwan, J.; Ulrich, S.; Batori, V.; Ehrhardt, H.; Silva, S. R. P. Raman spectroscopy on amorphous carbon films. *J. Appl. Phys.* **1996**, *80*, 440-447.
46. Ferrari, A. C. Raman spectroscopy of graphene and graphite: disorder, electron–phonon coupling, doping and nonadiabatic effects. *Solid State Comm.* **2007**, *143*, 47-57.